Cold Regions Science and Technology 101 (2014) 14–23

Contents lists available at ScienceDirect

Cold Regions Science and Technology

journal homepage: www.elsevier.com/locate/coldregions

Micromechanical analysis of deformation of snow using X-ray tomography

Chaman Chandel [a,b], Praveen K. Srivastava [a,b], P. Mahajan [b,*]

[a] Snow & Avalanche Study Establishment, Plot No 1, Sec-37, Chandigarh, India
[b] Applied Mechanics Department, IIT Delhi, Hauz Khas, New Delhi, India

ARTICLE INFO

Article history:
Received 28 June 2013
Accepted 24 January 2014
Available online 31 January 2014

Keywords:
Damage
Elastic modulus
Strain softening
Ultimate strength
Integral range

ABSTRACT

Snow exhibits an elastic response followed by a softening behavior under compression at a strain rate of $10^{-4}\ s^{-1}$ and higher. The strain softening behavior is postulated due to initiation and growth of damage in the ice matrix. A deformation controlled compression experiment at a strain rate of $2 \times 10^{-4}\ s^{-1}$ was conducted on a round grained snow sample. To investigate the link between behavior of snow and ice, X-ray tomographic imaging of the sample was performed and the size of representative volume element (RVE) with respect to ice volume fraction $\left(V_{\phi_i}^{RVE}\right)$ was estimated. From the set of scanned images 112 sub-volumes of sizes equal to and larger than $V_{\phi_i}^{RVE}$ were selected. The ice matrix formed by these images was meshed with finite elements (FE) to simulate the stress–strain curve of snow under deformation controlled compression. An elasto-plastic constitutive law for ice with provision for degradation of elastic modulus due to damage was used to simulate the stress–strain response including strain softening as observed in the experiment. The statistical representativeness of the RVE with respect to ultimate strength (S) and elastic modulus (E) of snow was further analyzed in terms of the precision of the numerical estimates of the effective properties. It was found that the standard deviation in the ultimate strength & elastic modulus is reduced by 50% for sub-volume of size 8 $V_{\phi_i}^{RVE}$ as compared to the sub-volume of size $V_{\phi_i}^{RVE}$. The sensitivity of overall stress–strain response to the finite size effects is also analyzed and the average coefficient of variation of the simulated stress–response with respect to the experimental response reduces from 44% for 5.745 mm^3 to 18% for 45.96 mm^3.

1. Introduction

Snow is a porous material with a solid skeleton or matrix of ice. The mechanical response of snow strongly depends on the morphology of the ice phase distribution in space. The ice matrix has a number of dead ends and only a small portion of it contributes to transfer of stress (Pinzer, 2009). The mechanical behavior of the ice matrix determines the mechanical behavior of snow, which in turn helps to understand the slab avalanche release mechanism. McClung (1987) studied strain softening response in snow under shear loading and found that the response depends on the applied deformation rate. The sintering and damage processes are simultaneously active in a natural snowpack under the effect of loading (Schweizer et al., 2003). As the deformation rate is increased, the damage processes, which are interpreted as microscopic failures at the scale of bonds, dominate the sintering effect (since finite time is needed for sintering to occur).

Various possible deformation mechanisms have been conjectured during the deformation process of snow, which includes: grain bond fracturing, sintering of grains (Voitkovsky et al., 1974) and intra-crystalline deformation by basal glide (Feldt and Ballard, 1966). Kry (1975) utilized stereology theory to characterize the inter-granular bonds of fine-grained snow and identified bonds and chains of grains as critical load carrying parts of the ice structure. Brown (1980) developed a volumetric constitutive relation based on a neck growth model where the neck is defined as a constricted region between ice grains. The model assumes that most of the deformation could be represented through compressive strains in the necks of the granular structure. Hansen and Brown (1986, 1988) utilized an internal state variable approach to describe the inelastic deformations in terms of an internal state vector which is represented by the mean inter-granular slip distance, mean grain size, mean bond radius, and the mean neck length. Mahajan and Brown (1993) modeled the inter-granular slip by allowing the necks to fracture at a critical neck stress. Below the critical neck stress, the deformation was modeled as elastic-viscoplastic flow and the global strain was calculated on the basis of these neck deformations. As a result, the local stresses/strains on the bond were almost an order of magnitude higher than the macroscopic stresses/strains. One major drawback of the above studies was that the idealized definitions of bonds and necks were used which were determined by using stereological principles (Gubler, 1978). Shapiro et al. (1997) concluded that critical parameters such as

* Corresponding author. Tel.: +91 11 26591229; fax: +91 11 26581119.
E-mail address: mahajan@am.iitd.ac.in (P. Mahajan).

0165-232X/$ – see front matter © 2014 Elsevier B.V. All rights reserved.
http://dx.doi.org/10.1016/j.coldregions.2014.01.005

bonds and necks cannot be established with sufficient accuracy by stereology due to inherent assumptions about the shape and isotropy of the microstructure.

The direct 3-D reconstruction of snow microstructure (Brzoska et al., 1999; Schneebeli and Sokratov, 2004) at resolutions down to a few microns is now possible with X-ray micro-computed tomography (μ-CT). Schneebeli (2004) demonstrated the potential of direct finite element simulations on the 3-D microstructure for the computation of the elastic modulus of temperature gradient metamorphosed snow; however the results were not correlated with the structural changes. Srivastava et al. (2010) studied the evolution of elastic properties during temperature gradient metamorphism using micro-CT and FE analysis. Yuan et al. (2010) computed the effective elastic properties using mesh free modeling from statistical reconstruction of 3-D snow micro-structure. Theile et al. (2011) described a first verified model of the macroscopic behavior of round grain snow based only on its microstructure and the properties of ice. One important step in this work was the approximation of the microstructure by beam elements to reduce the computational cost of the simulations. However, not all snow types can be represented by a network of beam elements. In a recent study, Schleef and Löwe (2013) conducted creep experiment on fresh snow and studied the densification and change in specific surface area (SSA) with deformation.

In the present work, unconfined constant strain rate test was conducted in a specially designed mechanical testing stage (MTS) to obtain the stress–strain response of a round-grained snow sample. The microstructure of the snow sample was obtained using μ-CT imaging. Our purpose was to model the strain softening behavior of snow using the real 3-D microstructure and damage properties of ice. A statistical computational approach proposed by Kanit et al. (2006) for random composites is adopted to investigate the precision of numerical estimates of the effective properties obtained using numerical simulation. We first briefly describe the experimental procedure and then describe the constitutive behavior and mechanical properties of ice used for finite element based simulations of macroscopic snow response. Finally, we present the results of numerical analysis.

2. Experimentation and methodology

2.1. Unconfined compression experiments

A series of unconfined deformation controlled compression experiments were conducted on round grain snow to discern the strain softening behavior in a cold room at Patsio research station (32 45′ N; 77 16′ E, 3800 ma.s.l.) in the Indian Himalayas. The cylindrical samples of 65 mm diameter and 150 mm length were directly extracted from a round-grained snowpack layer. A range of strain rates from 7.2×10^{-6} s^{-1} to 7.2×10^{-3} s^{-1} was selected for snow and the strain rates in the constricted regions are expected at least one order higher than the applied strain rates, which covers the transition zone from ductile to brittle behavior of polycrystalline ice (Schulson and Duval, 2009). The sample details and applied strain rates for five representative tests are given in Table 1. Fig. 1 shows the representative stress responses from these experiments at different strain rates. The stress–strain curves pertaining to samples C, D and E clearly indicate strain-softening behavior, as the applied strain rate is increased beyond 10^{-4} s^{-1}. These findings are similar to that reported by McClung (1987). The objective of showing these curves is to identify the strain rate at which strain softening is mostly observed. Based on these preliminary findings, we selected a strain rate of 2×10^{-4} s^{-1} to carry out micromechanical analysis.

Table 1
Experimental details.

Curve	Snow grain/density (kg/m^3)	Strain rate (s^{-1})	Strain hardening/softening
A	RGsr/270–290	7.2×10^{-6}	Hardening
B	RGsr/270–290	4.8×10^{-5}	Hardening
C	RGsr/270–290	4.8×10^{-4}	Softening
D	RGsr/270–290	7.2×10^{-3}	Softening
E	RGsr/240–250	4.8×10^{-4}	Softening

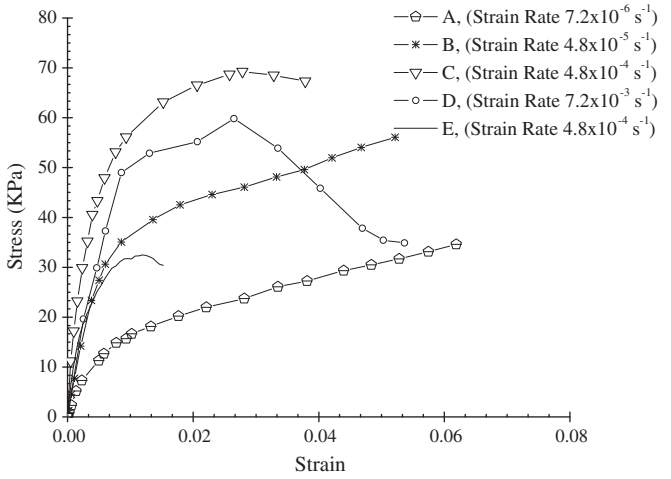

Fig. 1. Compressive stress–strain behavior of round grain snow under different strain rate applications from 7.2×10^{-6} s^{-1} to 7.2×10^{-2} s^{-1}.

In order to characterize the microstructure for micromechanical simulation studies, snow from the same round-grained snowpack layer was transported in an insulated box to an environmental chamber at Manali, (HP) India. A cylindrical snow sample of diameter 12.25 mm and height 17 mm was prepared using a sieve with 1.0 mm opening and stored at −20 °C for 24 h prior to imaging and mechanical testing. A specially designed SkyScan material testing stage (which can be fitted into the scanning chamber of the μ-CT system) was used to conduct the deformation controlled compression experiment (Fig. 2). The MTS of load capacity of 440 N is designed to apply controlled deformation at a fixed deformation rate of 0.2 mm min^{-1}. For the given sample dimension, this corresponds to a strain rate of approx. 2×10^{-4} s^{-1} and the stress response obtained in the MTS is shown in Fig. 3. The 3-D microstructure of the sample was imaged in the μ-CT system prior to the compression experiment.

2.2. X-ray microtomography imaging

The cylindrical snow sample was first weighed to calculate its density ($\rho_s = 257$ kg/m^3) and then was imaged with a SkyScan 1172 high resolution μ-CT system. The objective of X-ray absorption tomography was to reconstruct the 3D internal microstructure from the multiple X-ray shadow projection images recorded at different angular positions of the sample. In this work, 600 projection images covering 180° rotation around the vertical axis were obtained for the snow sample. The images were acquired at a resolution of 7.96 μm from the mid-height of the sample. From the projection images, a cubic volume corresponding to a physical side length of 7.164 mm was reconstructed using modified Feldkamp cone beam software (NRecon, SKYSCAN). The reconstructed 3-D images have an isotropic resolution of 7.96 μm, resulting in 900 images of 900 × 900 pixels, which is a considerable quantity of volumetric data for processing. The resolution of the 3-D images was reduced by a factor of 3 in the three directions (300 × 300 × 300 voxels) to reduce processing and computational time for the microstructure parameter determination and simulation of mechanical behavior. In all the results presented here, one voxel corresponds to 23.88 μm. The gray-level images were filtered with a 3^3 median filter prior to image reduction. As the gray-level images showed adequate contrast, an automatic threshold using the histogram